

# **DRI Internal Wave Simulations**

by Stephen A. Reynolds<sup>1</sup> and Murray D. Levine<sup>2</sup>

<sup>1</sup> *Applied Physics Laboratory, University of Washington, Seattle*

<sup>2</sup> *College of Oceanic and Atmospheric Sciences, Oregon State University, Corvallis*

Technical Memorandum

**APL-UW TM 5-04**

January 2005



**Applied Physics Laboratory University of Washington**  
1013 NE 40th Street Seattle, Washington 98105-6698

Contract N00014-98-G-0001

**BLANK PAGE**

## ***Acknowledgments***

We wish to thank the Uncertainty DRI Management Team of the Office of Naval Research for supporting our work in contribution to “Capturing Uncertainty in the Common Tactical/Environmental Picture.”

## ***Abstract***

The ocean is a stratified medium and thus filled with internal gravity waves. Even though the statistics of these fluctuations are fairly well known, these waves fluctuate randomly and hence represent true uncertainty. When an acoustic prediction is needed for an ocean region, knowledge of the background sound speed profile is an additional uncertainty. A processing module is developed that takes profile estimates as input and uses numerically simulated linear internal wave displacements to create two-dimensional range-dependent sound speed fields. These fields are available for use in acoustic modeling and target estimation studies. Field realizations were obtained for four ocean regions. These examples illustrate variability induced by internal waves and how this variability may be useful in some important ways.

## 1. Introduction

Making an acoustic prediction for an unknown or little known ocean environment is problematic. This is known as “predictive uncertainty” (*Wagener et al.*, 2004). Given today’s research assets, the goal of the Uncertainty DRI is to assess ocean uncertainty for the fleet, understand the inherent signal processing limits and learn how to reduce predictive uncertainty. A subsidiary goal is to recognize properties of ocean uncertainty that may be exploited. Within this context, uncertainty is defined as the error between reality and prediction.

Random motions from internal waves are ubiquitous in the ocean. Sound speed fluctuations induced by internal waves scatter acoustic energy; the acoustic fluctuations build up over range. The acoustic signals are perturbed randomly, hence these sound fluctuations represent true uncertainty.

A reasonable starting point in describing internal waves is the Garrett–Munk (GM) spectrum (*Munk*, 1981). This model was developed using deep water measurements but is also used in shallow water environments (for a discussion see *Levine*, 2002). In shallow water a non-WKB formulation must be used along with different parameters so that the predictions compare favorably with measurements (*Williams et al.*, 2001). *Winters and D’Asaro* (1991) developed a numerical code that simulates internal wave displacements using the GM framework. A modified version of their code is used here, with the WKB assumption removed, for the study of a variety of ocean scenarios.

Perturbed range-dependent sound speed profiles are the output of this processing. This work is one module in the processing chain of a group of DRI investigators. The module described here starts with an environmental background prediction, leads to a decision on background sound speed and density profiles, and then outputs perturbations of these profiles using the simulated internal wave displacements. These profiles become input to acoustic modeling modules that examine target strength uncertainty and target state estimation. A module may or may not be included in the processing chain; for example, internal waves may be excluded. In this modular approach, as new modeling capabilities develop, they can be inserted in the processing chain.

Section 2 describes the methodology in profile selection and internal wave simulation. Section 3 presents four scenarios, two shallow water and two deep water. The four were all accomplished under the Uncertainty DRI. Examining new scenarios is straightforward. The summary considers what steps could be taken next within the context of what has been learned. Although internal wave effects are random, these effects may be useful in some important ways.

## 2. Methods

Our approach is summarized as follows: (a) obtain input “background” density and sound speed profiles (or clusters of profiles) from the MODAS (Modular Ocean Data Assimilation System; see *Fox et al.*, 2002) or another database; (b) interpolate these profiles on a fine grid and estimate the buoyancy profile  $n(z)$ ; (c) establish parameters for the internal wave modeling, use  $n(z)$  to calculate internal wave modes and run simulation software to produce internal wave displacement fields in range and depth,  $\zeta(x,z;t)$ —(time is a parameter); (d) using  $\zeta(x,z;t)$  form a range/depth sound speed field  $c(x,z;t)$  and output this data for use in acoustic modeling modules.

### Environmental profiles

Buoyancy and corresponding sound speed profiles as functions of depth are needed. Ideally, these represent the ocean ‘background’; that is, the vertical fields unaffected by internal waves. Two climatological sources, the MODAS and Levitus databases, were used. MODAS is ideal because individual casts may be examined. It was clear that in both these databases, average profiles have important features smoothed out—mainly the sharp corner at the base of the mixed layer but also other features, such as interleaving of persistent water types.

The Levitus profiles for a given region and time of year are available from a website: <http://ingrid.ldeo.columbia.edu/SOURCES/LEVITUS94/oceanviews.html>. Dan Fox and others at the Naval Research Laboratory, Stennis provided data from MODAS. In the data development we realized that to maintain the features described above, a technique for obtaining representative individual profiles would be a better choice for the acoustic modeling than using data averaged profiles. The NRL Stennis group provided “cluster” analyses of individual temperature profiles from the MODAS database. Profiles were grouped (clustered) according to water type and then the median profile from each cluster was used in the modeling (Dan Fox, pers. comm.). Often, XBT or other data profiles do not extend over the full depth. In most scenarios, the climatological average profiles were used to extend the data over the full depth. Nevertheless, local data is preferred. For one of the scenarios, Seaglider (*Ericksen, et al.*, 2001) profiles were available and were utilized.

### Interpolation for modeling

The input profiles are sparsely sampled in depth. The simulations require a finely sampled data grid. In some cases both temperature and salinity were available allowing a straightforward sound speed and density calculation. If salinity was not available from MODAS, the salinity was inferred from temperature using an average TS relation from Levitus. From the sparsely sampled data, a spline technique was used to interpolate onto a uniform, finely sampled depth grid. The profiles were then low-pass filtered to remove high wave number variability. Typically, below the mixed layer, length scales smaller than 20–30 m were removed. The results are the background sound speed  $c_0(z)$  and density.

With the potential density sampled on a fine grid, the buoyancy profile was obtained by central difference

$$n(z) = -g/\rho \partial\rho/\partial z; \quad (1)$$

$\rho$  is the potential density and the differences are evaluated at  $z_+$  and  $z_-$ , with  $\partial z = z_+ - z_-$  and  $z = 0.5(z_+ + z_-)$ .  $z$  is positive-up. The  $n(z)$  profile allows us to calculate the vertical eigenmodes for the internal waves (see *Winters and D'Asaro, 1997*, for example). Except for the behavior near the mixed layer, internal wave displacements are not particularly sensitive to details of  $n(z)$  and it is assumed that an averaged density profile is sufficient. For the region of the mixed layer and thermocline, data from a single cast, typical of the region and time of year (e.g., the center cast of a cluster), was merged with deeper data taken from averaged MODAS or Levitus.

### Internal wave model parameters

The internal wave simulator is based upon *Winters and D'Asaro (1997)*. An important modification of their formulation is that the method used here does not rely on a WKB approximation. WKB is especially problematic in shallow water environments. (A detailed description of the formulation is available from the authors.) In addition to  $n(z)$ , there are two parameters needed to specify the spectrum. These include the mode bandwidth  $j^*$  and energy level  $bE_{GM}$  (*Munk, 1981*). The total number of vertical modes  $j_{\max}$  must also be specified. See *Heney et al. (1997)* for details of the spectral model. In all cases the energy level is set so that the displacement variance is consistent with observation; in the NORPAC and Hawaii cases, it equals the GM level of  $53 \text{ m}^2$  at the depth where  $n = 3 \text{ cph}$  (*Munk, 1981*). The numerical method uses a Monte Carlo technique to produce realizations of three dimensional fields of internal wave displacement,  $\zeta(x,y,z;t)$ . Several realizations are produced for each scenario. Each run of the program results in fourteen evolving time steps. In this case a large time step was used so that the field at one time was decorrelated from fields at other times and so each time may be used as an independent realization.

### Form $c(x,z;t)$

Displacement slices in range and depth,  $\zeta(x,z;t)$ , were obtained by subsampling the three-dimensional displacement fields. Using the sound speed profile a two-dimensional sound speed field is formed for use in the acoustic propagation modeling:

$$c_p(x,z;t) = c\theta_p(x,z - \zeta(x,z;t)). \quad (2)$$

The sound speed perturbation due to internal waves equals  $c_p - c\theta_p$ . These are potential sound speed profiles. For propagation modeling the adiabatic component must be included. The total (potential plus adiabatic) two-dimensional sound speed realizations are the output product from the internal wave modeling. Examples are described in the next section.

### 3. DRI scenarios

Four geographic locations were studied as part of the DRI. Two were downward refracting shallow water environments: a Mid-Atlantic Bight location and one in the East China Sea (ECS); and two were deep water environments: an eastern North Pacific (NORPAC) site (actually two nearby sites with experiments in 2003 and 2004) and an area near Hawaii (RIMPAC).

#### Mid-Atlantic Bight

Water depth at the Mid-Atlantic Bight location ( $39.25^\circ\text{N}$ ,  $72.4^\circ\text{W}$ ) was 200 m with a sandy bottom. For the acoustic geometry a point source at 50 m with 20 km range was assumed. NRL Stennis provided density and sound speed profiles from the MODAS database for a 1 September climatology. Casts were identified and checked for T/S consistency.

Sound speed and buoyancy frequency profiles are shown in Figure 1. The peak in  $n(z)$  of 31 cph (both its value and depth) is important as is the small duct in sound speed at 60 m depth. To specify the internal wave model,  $j^* = 1$ . The modal bandwidth is known to be low in shallow water and the depth integrated energy level is about half the GM level. These values were determined north of the SWARM area during an earlier experiment (*Williams et al.*, 2001). For the simulator two maximum mode numbers,  $j_{\max} = 50$  and 100, were used for this trial. This was done to examine the effect of higher vertical wave numbers on the acoustics statistics. Higher  $j_{\max}$  leads to longer run times;  $j_{\max} = 40$  or 50 is typical.

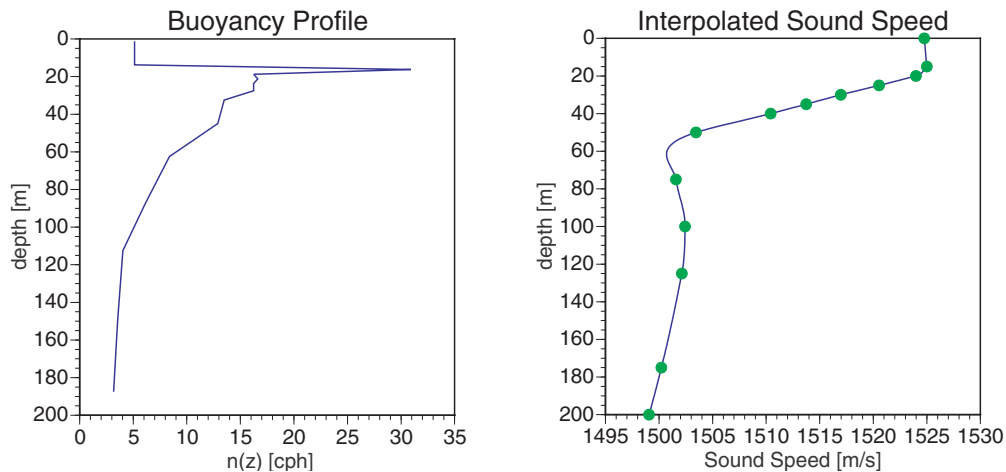


Figure 1. Input buoyancy (left) and inferred sound speed (right) for the Mid-Atlantic Bight Scenario. Measured sound speed values are shown as green dots.

Ten separate realizations were run for the Monte Carlo and within each, displacement fields were created for 14 different times with the time separation long enough that the fields were uncorrelated. This raised the number of effectively independent realizations to 140. Example fields of displacement and associated sound speed perturbation are shown in Figure 2.



While larger displacements are found deeper, the larger sound speed perturbations, obtained using (2), are concentrated in the depth range where sound speed gradients are higher.

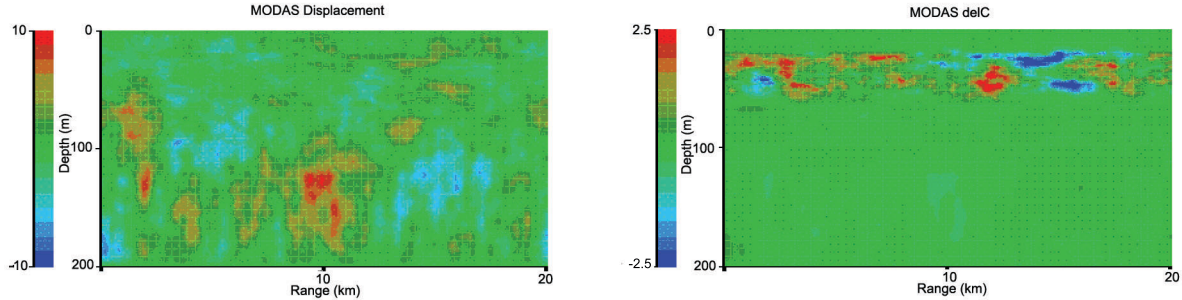


Figure 2. Example (20 km by 200 m) range/depth slices from the Mid-Atlantic Bight scenario. Internal wave displacement (left) and associated sound speed perturbation (right).

Sample PE runs were made using both the background and internal wave perturbed sound speed fields. Two intensity (TL) fields, one with internal wave variability and one without, are shown in Figure 3 for a 3-kHz point source. There are two observations of note. First, the internal waves produce focusing regions (e.g., the bright spots near 10.5 km at mid-depth). This property is well known (see *Potter et al.*, 2000). The temporal/spatial properties in shallow water of these 5–10-dB “hot spots” were not determined, and whether they are exploitable for detection remains a question. Second, the field down range appears cleaner; this is likely due to the known effect of randomness coupling energy into higher modes, which are then absorbed in the sediment. In testing the effect of varying  $j_{\max}$ , no change in the average properties of the transmission loss were observed. Changes in the tails of the distributions, however, may occur.

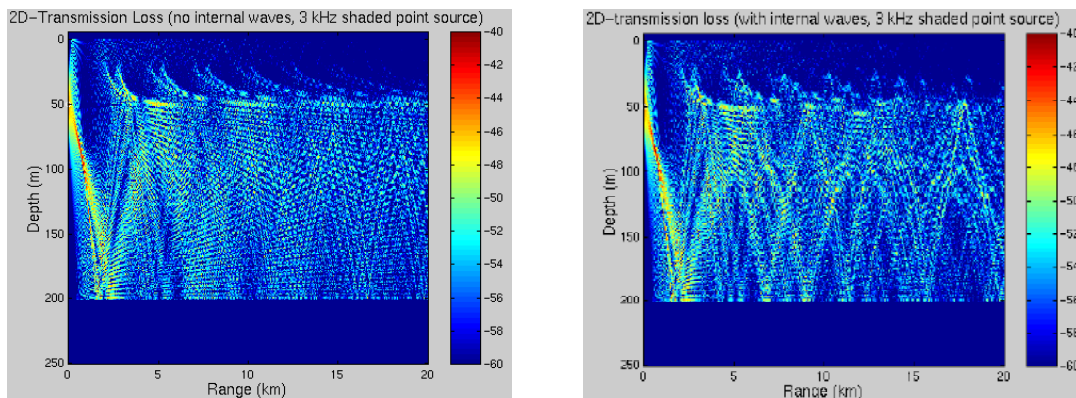


Figure 3. PE transmission loss fields with no internal waves (left) and with internal waves (right).

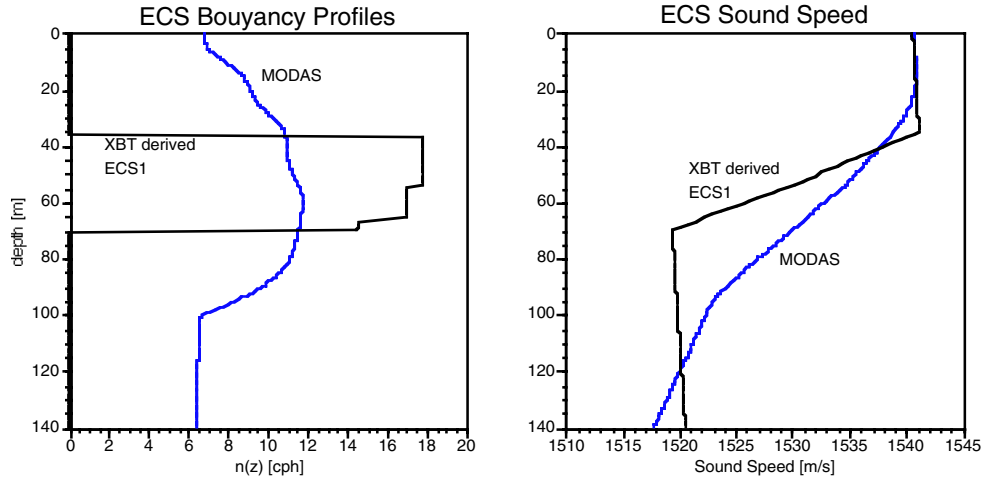


Figure 4. Buoyancy and background sound speed profiles for the East China Sea region from the MODAS database (blue) and an XBT derived profile (black).

### East China Sea (ECS)

The other shallow water site considered was a location in the East China Sea (29.7°N, 126.8°E). A 140-m water column lies over a silty/sandy bottom. For this situation a study of the importance of different sound speed profiles was made with the internal wave simulations. A ship traversing a site has two options. They may either use an average profile, e.g., MODAS climatology, or take an XBT(s) and infer a background profile. Five different profiles, plausible for the date and location, were considered. An averaged profile from the MODAS data set was provided by NRL Stennis. Also, four possible single cast profiles were derived from local XBT casts and modeled as a surface and a bottom mixed layer separated by a high gradient region. MODAS and one of four XBT inferred profiles are shown in Figure 4 along with the associated buoyancy profiles.

The internal wave model parameters were the same as for the Mid-Atlantic Bight except a single  $j_{\max}$  of 50 was used. Again, many (112) independent realizations were obtained via numerical simulation. Example perturbation fields from the two sound speed profiles are shown in Figure 5. A ray from a point source at 7.6 m to a range of 15 km is overdrawn. This path was used to sample intensity statistics. The XBT profile perturbations are confined in depth relative to those of MODAS.

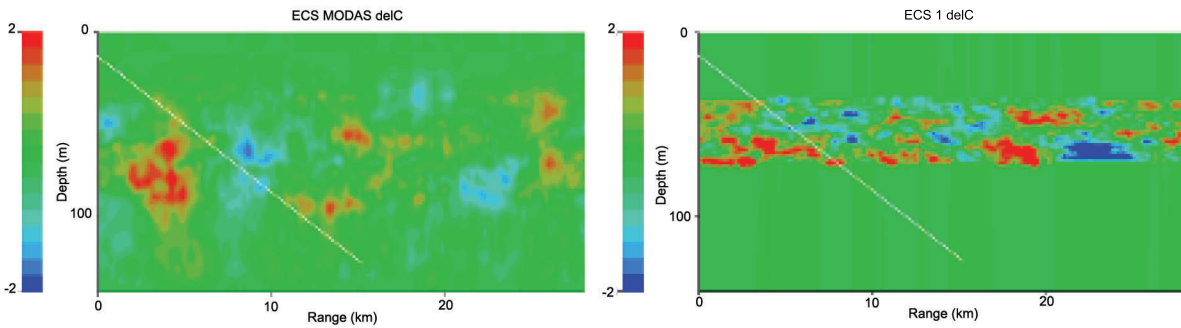


Figure 5. Sound speed perturbations for MODAS (left) and XBT-derived ECS1 (right) profiles. Slices are 140 m deep and 28 km in range.

PE runs (*RAM*; Collins, 1993) were made using the ECS sound speed fields with internal waves. The bottom was modeled as uniform with a sound speed of 1585 m/s, a bottom density of 1.85 times that of the water, and an attenuation of 0.5 dB/ $\lambda$ . Data from all five sound speed situations were used and average transmission loss (TL) was obtained along the ray paths. The resulting statistics show that in general, the XBT derived profiles were not statistically different from each other. But the MODAS profile produces average TL curves different from the XBT derived cases. To be more specific, within the geometry studied, over the first 5 km of the ECS transmission path, the internal waves do not change the predictability for average intensity. From 5 to 15 km, the internal waves on average fill in fades and smooth peaks of range independent profiles so that TL curves for similar XBT derived profiles exhibit the same statistics. The differences in sound speed profile are typical of what may be observed over a 10–20-km range where there are no fronts. This implies that within 20 km, the presence of internal waves makes small profile differences less important to predicting TL statistics. However, using the average MODAS profile does not produce TL statistics representative of those from the XBT even in the presence of internal waves. We conclude that local knowledge of the sound speed profile is necessary to reduce predictive error. Within a range of 10 to 20 km, only a few profiles should be necessary to reduce uncertainty and improve predictability.

## NORPAC

In shallow water the seasonal profiles studied exhibit downward refracting sound environments. In these situations bottom characteristics will be important. In deep water the bottom tends to be less of an issue. Sound tends to stay in the duct in deep water columns, and in particular when sound speeds at the source are less than at the bottom.

Two scenarios in the northeast Pacific were considered—the first for an exercise in 2003 and a second nearby in 2004. For the March 2003 case NRL Stennis employed “cluster” analyses of sound speed databases for the location of the exercise (44°N, 135°W). Sound speed profiles are grouped by type in this analysis. The median profiles from each of three clusters were obtained. Monthly Levitus sound speed profiles were also utilized and the NRL Stennis profiles were extended to the deep ocean using them. Cluster analysis was not conducted for the

2004 case and only Levitus data for the month was used. The four possible sound speed profiles for 2003 and the single profile for 2004 are shown in Figure 6 along with the buoyancy profiles.

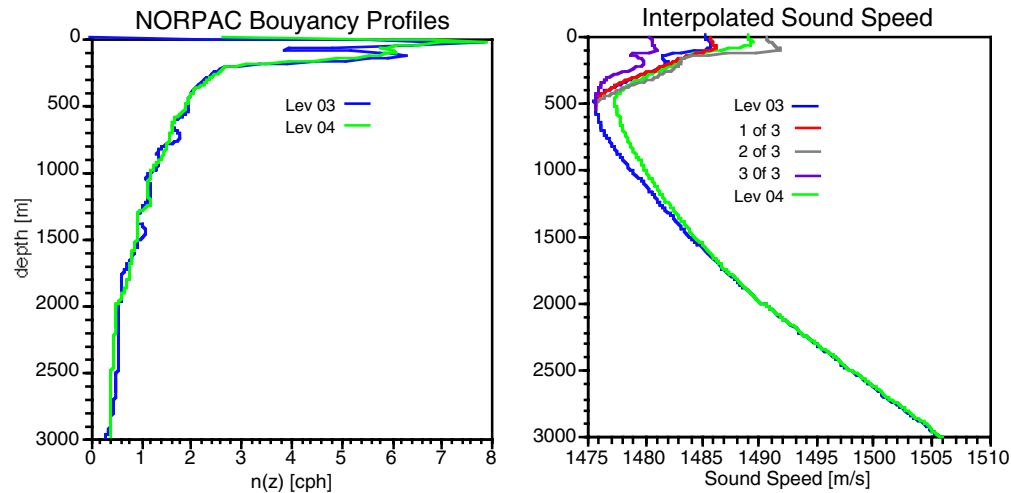


Figure 6. NORPAC buoyancy and sound speed profiles. Levitus data is for the appropriate month for each year and location. Three profiles from cluster analysis for 2003 were extended using Levitus. Two of the three and Levitus exhibit a duct at 150 m.

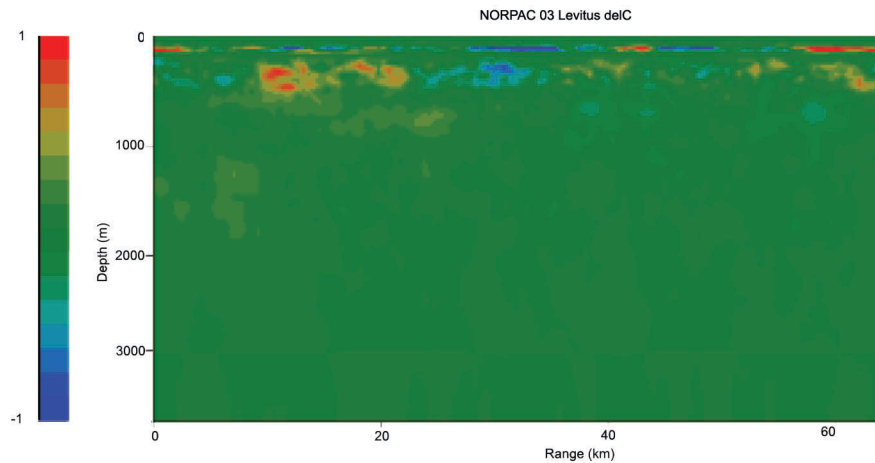


Figure 7. Sound speed perturbations over a 64-km range for the NORPAC 03 scenario. Depth is 3500 m. The gradients in a shallow duct produce a line of perturbations.

These cases again demonstrate the importance of knowledge of the profile in the upper ocean. Note the duct between 100 and 200 m in the 03 profiles. This apparently is a persistent feature (blue is Levitus climatology for March). However, there are times during apparent surface warming when this feature is not present (profile 2 of 3). The sound speed perturbation for one of the duct features in the NORPAC 03 scenario is shown in Figure 7. The presence of the duct produces a line of significant perturbations in addition to the changes seen in the deeper

thermocline. Canonical GM parameter values (*Munk*, 1981) were used for these deep water simulations with  $j_{\max}$  set to 40; 70 realizations were produced for each year.

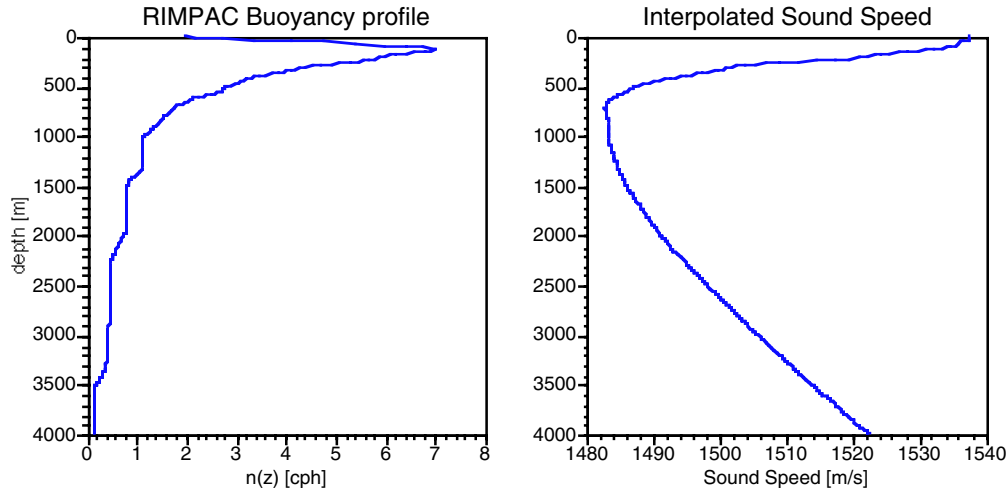


Figure 8. RIMPAC (19.5°N, 157.5°W) profiles of buoyancy and sound speed.

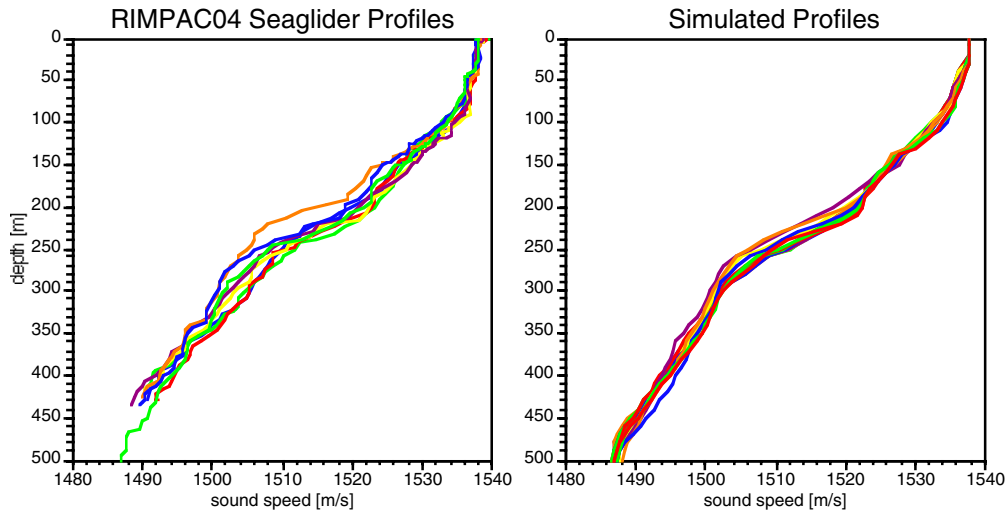


Figure 9. Sound speed profiles observed by Seaglider (left) and profiles given by (2) for internal wave displacements (right) simulated over a 10.7-hr interval.

## RIMPAC

A region west of Hawaii was the last area of interest. This exercise involved use of an APL-UW Seaglider and many sound speed profiles were available. A composite using a median profile from Seaglider was merged with July Levitus climatology data. The sound speed and density profiles are shown in Figure 8.

Seventy realizations of sound speed depth/range slices were obtained via simulation with the average internal wave displacement variance set to  $53 \text{ m}^2$  at the depth where  $n(z) = 3 \text{ cph}$  and  $j^* = 3$  (GM values). Figure 9 displays Seaglider profiles along with profiles from the numerical simulations. The simulations of course do not contain water mass changes. Except for a single Seaglider outlier cast, comparison is good. Figure 10 displays a sound speed perturbation field for one of the realizations. Significant perturbations are confined to regions of high sound speed gradient above 700 m depth.

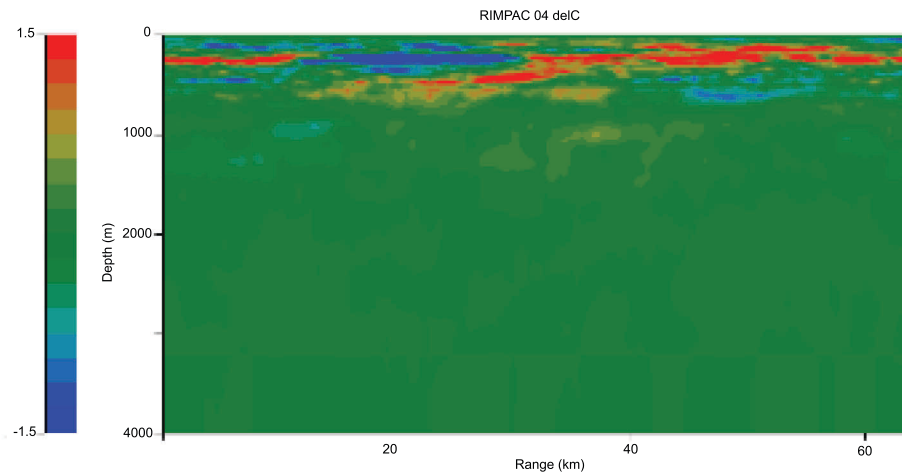


Figure 10. A RIMPAC sound speed perturbation field.

## 4. Summary

Random background internal waves are ubiquitous in the ocean. They are a persistent scatterer of acoustic energy. In four scenarios we have described simulations that produce underwater sound speed changes induced by internal waves. These data sets are used to study the predictability of underwater acoustic statistics, source detectability, and location by other DRI investigators.

### What have we learned?

- Careful treatment of the background sound speed profile is important in reducing “predictive uncertainty” (*Wagener et al.*, 2004). Local *in situ* measurements produce better outcomes. Either using a local XBT or taking clusters from the regional database to get a range of probable environments is generally preferable to using a long-term climatological average. The local XBT data and/or clusters provide enough knowledge to obtain profiles over the full depth by extending the local casts, which tend to be shallow, with monthly Levitus or MODAS data. These databases also provide a reasonable salinity estimate. Knowledge of the sound speed profile also improves estimates of the internal wave sound speed perturbation statistics.
- Internal wave variability in the East China Sea case made precise knowledge of local changes in sound speed profile less of an issue when sound propagates over ranges of less than a few tens of kilometers. The fluctuations filled in the nulls and smoothed out peaks in TL range curves so that the average TL was similar. Internal waves make the environmental determination less difficult by randomizing interactions. A similar effect occurs with bottom scatter where internal waves randomize ensonified spots on the bottom (*Rouseff and Ewart*, 1995).
- The random range dependent field produces focusing regions that may be useful in detection. Also, internal waves over an absorbing bottom scatter energy from low modes to high modes that are then absorbed. This process reduces complexity of the down range acoustic field.
- Finally, the uncertainty due to the internal waves is pervasive. But simulation of internal waves is numerically straightforward and including their effect in propagation codes has been demonstrated. Accuracy of simulated profile variability was qualitatively shown by comparison with Seaglider casts.

### Deliverables

- The three-dimensional internal wave code is available with run times on the order of tens of minutes to a few hours depending upon parameter choices. Other tools (e.g., to create perturbed sound speed profiles) are also available.
- The sound speed fields simulated for the various experiments are available.

### **New initiatives**

- Determine if temporal and spatial properties of internal wave induced “hot spots” are useful for detection
- Averaging smoothes important features out of historical sound speed profiles; better techniques for obtaining background profiles from databases are needed
- A two-dimensional internal wave model with shorter run times is available but needs modification for this use
- The effect of varying some internal wave model parameters were made, however, further examination would be helpful



## 5. References

- Collins, M. D., A split-step Pade' solution for the parabolic equation method, *J. Acoust. Soc. Am.*, **93**, 1736–1742 (1993).
- Ericksen, C. C., T. J. Osse, R. D. Light, T. Wen, T. W. Lehman, P. L. Sabin, J. W. Ballard, and A. M. Chiodi, Seaglider, a long-range autonomous underwater vehicle for oceanographic research, *IEEE J. Ocean. Eng.*, **26**, 424–436 (2001).
- Fox, D. N., W. J. Teague, C. N. Barron, M. R. Carnes, and C. M. Lee, The modular ocean data assimilation system (MODAS), *J. Atmos. Ocean. Technol.*, **19**, 240–252 (2002).
- Henye, F., D. Rouseff, J. Grochocinski, S. Reynolds, K. Williams, and T. Ewart, Effects of internal waves and turbulence on a horizontal aperture sonar, *IEEE J. Ocean. Eng.*, **22**, 270–280 (1997).
- Levine, M. D., A modification of the Garrett–Munk internal wave spectrum, *J. Phys. Oceanogr.*, **32**, 3166–3181 (2002).
- Munk, W. H., Internal waves and small-scale processes, in *Evolution of Physical Oceanography*, B. A. Warren and C. Wunsch, eds., MIT Press, 264–291 (1981).
- Potter, J. R., B. J. Uscinski, and T. Akal, Random focusing of sound into spatially coherent regions, *Waves in Random Media*, **10**, 199–216 (2000).
- Rouseff, D. and T. E. Ewart, Effect of random sea surface and bottom roughness on propagation in shallow water, *J. Acoust. Soc. Am.* **98**, 3397–3404 (1995).
- Wagener, T., M. Sivapalan, J. McDonnell, R. Hooper, V. Lakshmi, X. Liang, and P. Kumar, Predictions in ungauged basins as a catalyst for mutlidisciplinary hydrology, *EOS Trans. AGU*, **85**, 451 ff. (2004).
- Williams, K. L., F. S. Henye, D. Rouseff, S. A. Reynolds, T. E. Ewart, Internal wave effects on high-frequency acoustic propagation to horizontal arrays—Experiment and implications to imaging, *IEEE J. Ocean. Eng.*, **26**, 102–112 (2001).
- Winters, K. B., and E. A. D'Asaro, Direct simulation of internal wave energy transfer, *J. Phys. Oceanogr.* **27**, 1937–1945 (1997).

**BLANK PAGE**

REPORT DOCUMENTATION PAGE			Form Approved OPM No. 0704-0188	
Public reporting burden for this collection of information is estimated to average 1 hour per response, including the time for reviewing instructions, searching existing data sources, gathering and maintaining the data needed, and reviewing the collection of information. Send comments regarding this burden estimate or any other aspect of this collection of information, including suggestions for reducing this burden, to Washington Headquarters Services, Directorate for Information Operations and Reports, 1215 Jefferson Davis Highway, Suite 1204, Arlington, VA 22202-4302, and to the Office of Information and Regulatory Affairs, Office of Management and Budget, Washington, DC 20503.				
1. AGENCY USE ONLY (Leave blank)		2. REPORT DATE January 2005		3. REPORT TYPE AND DATES COVERED Technical Memorandum
4. TITLE AND SUBTITLE UDRI Internal Wave Simulations			5. FUNDING NUMBERS N00014-98-G-0001	
6. AUTHOR(S) Stephen A. Reynolds and Murray D. Levine				
7. PERFORMING ORGANIZATION NAME(S) AND ADDRESS(ES) Applied Physics Laboratory University of Washington 1013 NE 40th Street Seattle, WA 98105-6698			8. PERFORMING ORGANIZATION REPORT NUMBER TM 5-04	
9. SPONSORING / MONITORING AGENCY NAME(S) AND ADDRESS(ES) Douglas Abraham, Code 321US Office of Naval Research 800 N. Quincey Street Arlington, VA 22217-5660			10. SPONSORING / MONITORING AGENCY REPORT NUMBER	
11. SUPPLEMENTARY NOTES				
12a. DISTRIBUTION / AVAILABILITY STATEMENT  Approved for public release; distribution is unlimited.			12b. DISTRIBUTION CODE	
13. ABSTRACT (Maximum 200 words)  The ocean is a stratified medium and thus filled with internal gravity waves. Even though the statistics of these fluctuations are fairly well known, these waves fluctuate randomly and hence represent true uncertainty. When an acoustic prediction is needed for an ocean region, knowledge of the background sound speed profile is an additional uncertainty. A processing module is developed that takes profile estimates as input and uses numerically simulated linear internal wave displacements to create two-dimensional range-dependent sound speed fields. These fields are available for use in acoustic modeling and target estimation studies. Field realizations were obtained for four ocean regions. These examples illustrate variability induced by internal waves and how this variability may be useful in some important ways.				
14. SUBJECT TERMS internal waves, numerical simulations, underwater acoustics, environmental uncertainty			15. NUMBER OF PAGES 15	
			16. PRICE CODE	
17. SECURITY CLASSIFICATION OF REPORT  Unclassified	18. SECURITY CLASSIFICATION OF THIS PAGE  Unclassified	19. SECURITY CLASSIFICATION OF ABSTRACT  Unclassified	20. LIMITATION OF ABSTRACT  SAR	